

Tuning of Au/n-GaAs Diodes with Highly Conjugated Molecules

Deng Guo Wu,[†] Jamal Ghabboun,[†] Jan M. L. Martin,[‡] and David Cahen^{*,†}

Department of Materials and Interfaces, and Department of Organic Chemistry, Weizmann Institute of Science, Rehovot, 76100 Israel

Received: July 13, 2001; In Final Form: September 7, 2001

Bifunctional conjugated molecules, consisting of electron donating or accepting groups that are connected, via a conjugated bridge, to a carboxylic acid group, were adsorbed as monomolecular carboxylate films on n-GaAs (100) and characterized by reflection FTIR, ellipsometry, and contact angle techniques. The way the donors and acceptors affected the electronic properties of the semiconductor was investigated. In agreement with theory, we find a linear relation between the calculated dipole moment of the molecules and the change in electron affinity of the molecularly modified surface, as well as between the barrier height of Au/molecule on n-GaAs junctions, extracted from their current–voltage characteristics and the dipole moment. The experimental results show little effect of the nature of the conjugated bridge in the molecules. Comparison with earlier work shows a clear decrease in the effect of the dipole of the free molecule on the semiconductor surface and interface behavior, notwithstanding the strongly conjugated link between the donor or acceptor groups of the molecule and the semiconductor surface. The simplest way to understand this is to consider the higher polarizability of the intervening bonds. Such effect needs to be considered in designing molecules for molecular control over devices.

Introduction

Although molecular organic (semi)conductors have been studied for more than fifty years, we are far from understanding them as well as we do their nonmolecular counterparts. Much work was and is done to use molecular organic semiconductors as the active component in (opto)electronic and electrooptical devices.^{1–3} Photovoltaic devices, using organics have been fabricated with, for example, conjugated polymers such as polyacetylene, poly(N-vinylcarbazole), and various derivatives of polyacetylene. Much of the recent interest is in molecular and polymeric organic or organic-based light-emitting devices.^{4–6} A major driving force in this area is the continuous quest to free microelectronics from the limitations imposed on it by Si and III–V technologies.⁷

Indeed, large efforts are made toward fully molecular electronics, including use of individual molecules as switches or memory units.⁸ We are pursuing a hybrid approach, using molecules to extend the properties of conventional semiconductors, and in this way to use the advantages of both. The idea is to control the electronic properties of semiconductor devices, via molecular control over the interface(s) in such devices. To do so, semiconductor or metal surfaces are modified by adsorbing molecules on the free surface, which can subsequently be made into an interface when it is used to make a device.⁹

The efficacy of such molecular control is assessed by using series of molecules, rather than a single type. In that series, a property (mostly we have used the dipole moment) is varied systematically. We then search for a corresponding systematic trend in semiconductor and device properties. This approach circumvents the problem of basing observations of a molecular

effect on comparisons of a system with a molecule to one without one.

Mostly the molecules that are used are composed of a binding group, a group with variable dipole, and a bridge that connects those.^{10–13} If the molecules form at least a partial monolayer on the surface of the solid (in our work we find generally between 0.75 and 1 monolayer^{14–17}), the resulting dipole layer will affect the work function of the molecularly modified solid. For a semiconductor, the relevant quantities are the electron affinity and the band bending (built-in potential). Changes in electron affinity can come about without charge transfer or polarization of the bond of the molecule with the solid's surface atoms, based just on the intrinsic dipole moment of the molecules [cf. Figures 4 and 5 in ref 18]. If charge transfer does occur, additional modifications take place (see below, discussion of Table 3 and Figure 5).

Figure 1 illustrates how dipole layers can affect the energetics at n-GaAs surfaces and interfaces. Figure 1a represents a situation of the energy profiles for bare n-GaAs contacted by a metal. Figure 1b,c shows the effect of a monolayer of adsorbed molecules on the electron energetic properties of the surface and interface. If molecules with a donor group at the end opposite the binding group are adsorbed on the semiconductor (Figure 1b), the work function (ϕ_s) and effective electron affinity (χ_s) of the semiconductor will decrease. This means that after adsorption of the molecule less external energy needs to be provided (as in a UPS experiment) than before to take an electron from the solid through the surface to a point just outside the range of the crystal forces. If molecules with an acceptor group are adsorbed (Figure 1c), the effective electron affinity (χ_s) and the work function (ϕ_s) will increase; that is, it will cost more energy to remove an electron from the surface, than if no molecules were present. As the surface becomes an interface, the *opposite* effect is obtained; that is, if molecules with an acceptor group are adsorbed on the semiconductor

* To whom correspondence should be addressed.

[†] Department of Materials and Interfaces, Weizmann Institute of Science.

[‡] Department of Organic Chemistry, Weizmann Institute of Science.

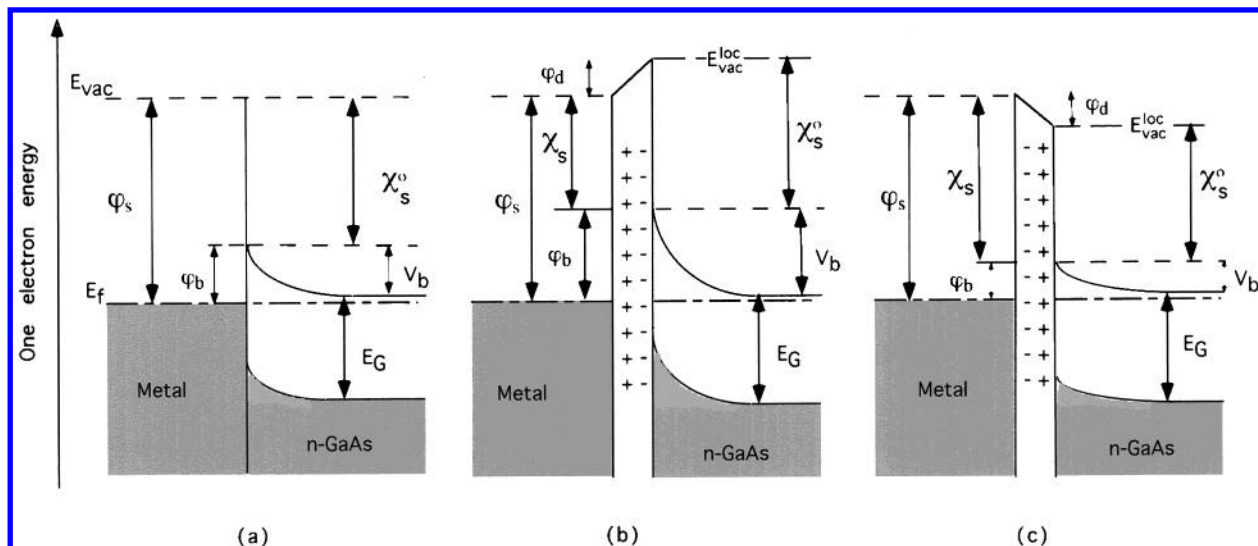


Figure 1. Different situations of the interfacial energy profiles at the n-GaAs/metal contact. (a) Bare n-GaAs, (b) with a monolayer of donor molecules, (c) with a monolayer of acceptor molecules adsorbed on the GaAs. $q\phi_b$: barrier height. qV_b : band bending (q is the electron charge). ϕ_s : work function. χ_s : electron affinity (for χ_s^o and ϕ_d , see eq 3). E_G : energy gap. E_F : Fermi level. E_{vac} : vacuum level, i.e., energy of an electron at infinity. E_{vac}^{loc} : local vacuum level, i.e., energy of electron just outside the range of crystal forces of the solid (cf. ref 54).

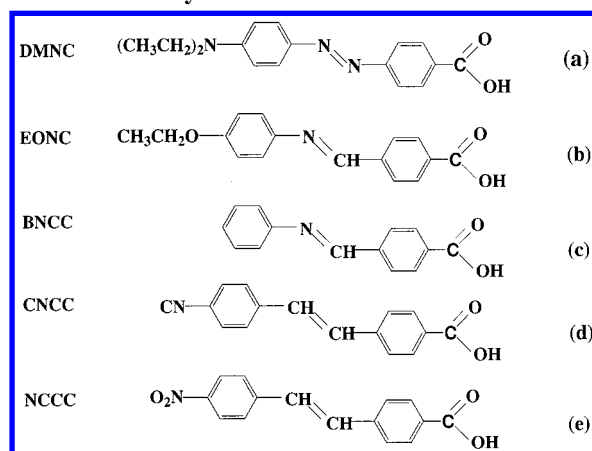
(Figure 1c), it will cost less energy to take an electron from the semiconductor to the metal. For free surfaces, these conclusions were verified on both metals^{15,19} and semiconductors^{14–16,20,21} for a number of molecular systems with bridges that were at least partially σ -bonded. The interfacial molecular dipole effect on device performance, as depicted in Figure 1, was recently verified by us^{10,22} and others²³ experimentally.

The effect of a layer of dipoles (as opposed to that of an isolated dipole) on the electrical potential of a semiconductor surface onto which the layer sits, has been treated theoretically^{24,25} (for metallic surfaces, cf. ref 19). Such an effect can be a long distance, rather than a local one.¹⁸ This is important as it allows for “action at a distance” of the molecules, thereby obviating the need for electron transport through the molecules and thus circumventing the issue of molecule stability. This is especially important if nonideal monolayers, i.e., layers with pinholes, are used.

The dipole effect will be operative as long as the molecular film has at least an average order, so as to display an average net dipole. Such order is assured by the average orientation of the dipolar group with respect to the binding group (and, thus, with respect to the solid surface). Therefore, and in contrast to other approaches to molecule-based electronics, there is no need for perfect, or near-perfect, packing of the molecules: such packing may even be detrimental for clear observation of the dipole effect. This is so because electron transfer across this type of molecularly modified interface will primarily be direct via pinholes, rather than via the molecules. This is important, as it leads to requirements in terms of molecules quite different from those for systems where the molecules need to form perfect monolayers or need to function as electronic conductors.

This then leads to the question in how far the nature of the bridge influences the molecules’ effects on the solid’s electronic properties, i.e., in how far will conjugated molecules differ from σ -bonded ones, in terms of the dipole effect. On one hand conjugated molecules are more easily polarized than σ -bonded ones, and indeed, a case has been made for use of conjugated bridges²⁶ in molecule-based electronics systems. However, one can also argue that conjugation, by increasing the effective dielectric constant (increasing the molecular polarizability), will decrease dipolar effects (see also eq 4, below).

SCHEME 1: Molecular Structures of the Molecules Used in This Study



In principle, the size of the dipole/unit area on a surface results from two contributions, the intrinsic dipole of the adsorbed molecules and charge transfer between the substrate and the adsorbate. The charge-transfer ability of the molecule can be expected to be different for conjugated and nonconjugated systems. Although electronic conduction through conjugated molecules has been studied extensively,^{27–31} the relevance of such results to their effect as surface modifiers is not obvious.

To study the importance of the bridge for the efficacy of molecular dipoles to tune semiconductor electron affinities, we designed and synthesized a series of bifunctional conjugated molecules (see Scheme 1), in which the anchoring groups for chemisorption to the solid surface are carboxylic acids. These molecules are based on similar ones, synthesized, and used for their photoelectric conversion activity.^{32,33} As functional groups, we introduced electron-withdrawing (acceptor) or electron-donating (donor) groups, opposite the binding group, and connected them by a conjugated system. Such molecules should be comparable to each other as all are conjugated, are planar, and have a trans structure. As semiconductor surface, we chose n-GaAs (100), because of the substantial experience we have working with it^{11–13} and because data on Au/GaAs diodes exist using series of nonconjugated molecular surface modifying

molecules.¹⁰ In this way, we can compare the extent of a systematic effect rather than effects of isolated molecules.

Experimental Section

1. Materials and Apparatus. The starting materials (4-bromobenzonitrile, 1-bromo-4-nitrobenzene, and 4-vinylbenzoic acid; *N,N*-diethylaniline and 4-aminobenzoic acid; *p*-phenetidine, aniline, and 4-carboxybenzaldehyde) were commercially available. Solvents used for molecular adsorption were HPLC or spectroscopic grade. Rinsing solvents were analytical grade or better. GaAs (100) wafers were purchased from AXT Co. Fourier transform infrared (FTIR) spectra were measured using a Bruker IFS66 instrument. Thin film thickness values were estimated by single wavelength (632.8 nm), variable angle ellipsometry. Contact angles, using water as solvent, were measured with a Rame-Hart goniometer. Current–voltage characteristics of Au/(molecule-on-GaAs) devices (for their preparation, see below) were obtained using a measurement system composed of a Keithley 486 picoammeter, Keithley 230 programmable voltage source, controlled by home-written software, using LabView (National Instruments). The point contacts between a W needle and the Au pads (see below) were controlled by a Nikon Optiphot optical microscope, equipped with CCD + video camera module. Contact potential differences (CPD) between the molecularly modified n-GaAs surfaces and a Au grid as reference were measured using a Kelvin probe apparatus (Besocke Delta-Phi, Juelich, Germany). Electron affinities and band bending values were extracted from measurements under photosaturation conditions and by comparing these with the results obtained in the dark.^{14,16}

2. Synthesis. Stilbene Compounds. A 100 mL flask was loaded under N₂ with 556 mg (3.1 mmol) of 4-bromobenzonitrile, for CNCC (614 mg (3.1 mmol) of 1-bromo-4-nitrobenzene, for NCCC), 452 mg (3.1 mmol) of 4-vinylbenzoic acid, 70 mg (0.06 mmol) of tetrakis-(triphenylphosphine)palladium(0), 6 mL (46 mmol) of triethylamine, and a Teflon-coated stir bar. A total of 30 mL of DMF, that were first dried for two weeks by molecular sieve type 4A, were added. The reaction mixture was heated to 130 °C for 13 h by an oil bath. The product was precipitated by addition of 2 N HCl to the reaction mixture and washed with boiling ethanol.³⁴

CNCC: Yield, 551 mg (74%); ¹H NMR (DMSO-*d*₆), δ = 7.46 (d, CH=CH, *J* = 4.43 Hz, 2H), 7.73 (d, phenyl-COOH, *J* = 8.21 Hz, 2H), 7.80 (m, phenyl-COOH, 2H, phenyl-CN, 2H), 7.90 (d, phenyl-CN, *J* = 7.93 Hz, 2H); MS, *m/z* (%) 248.04 (40%) [M–H][–], 204.00 (100%) [M–COOH][–]. NCCC: Yield, 511 mg (63%); ¹H NMR (DMSO-*d*₆), δ = 7.54 (d, CH=CH, *J* = 3.72 Hz, 2H), 7.74 (d, phenyl-COOH, *J* = 8.41 Hz, 2H), 7.89 (d, phenyl-COOH, *J* = 8.9 Hz, 2H), 7.93 (d, phenyl-CN, *J* = 8.2 Hz, 2H), 8.23 (d, phenyl-CN, *J* = 8.85 Hz); MS, *m/z* (%) 268.05 (50%) [M–H][–], 224.02 (100%) [M–NO₂–H][–].

Ethyl Red (DMNC). *N,N*-diethylaniline (2 mL, (=12.5 mmol) was kept below 5 °C in an ice bath. 4-aminobenzoic acid (1.65 g, 12 mmol) was dissolved in 20 mL of ethanol (including 2 mL of acetic acid) and cooled quickly to a temperature below 5 °C. Sodium nitrite (1 g, 14 mmol) in 2 mL of water was slowly dropped in the 4-aminobenzoic acid solution. After vigorous stirring at 0–5 °C for 30 min, a yellow suspension was obtained. The *N,N*-diethylaniline was added slowly to this suspension, while stirring. The mixture was stirred for half an hour and then neutralized with saturated aqueous solution of sodium carbonate. A red product precipitated out from the solution and was collected by filtering.³⁵ The product was recrystallized from methanol. ¹H NMR (DMSO-*d*₆), δ = 1.09 (t, 2CH₃, 6H), 3.36

(m, 2CH₂, 4H), 6.70 (d, phenyl-COOH, *J* = 8.1 Hz, 2H), 7.68 (m, phenyl-N, 4H), 7.96 (d, phenyl-COOH, *J* = 8.1 Hz, 2H); MS, *m/z* (%) 296.07 (100%) [M–H][–], 593.26 (5%) [2M–H][–].

Schiff Base Derivatives. The Schiff base derivatives were synthesized by the condensation of 4-carboxybenzaldehyde with the corresponding phenylamino derivative in the presence of an acid catalyst.³⁶ The compounds were recrystallized from methanol.

EONC: ¹H NMR (DMSO-*d*₆), δ = 1.28 (t, CH₃, 3H), 3.97 (m, CH₂O, 2H), 6.91 (d, phenyl-O, *J* = 8.90 Hz, 2H), 7.26 (d, phenyl-O, *J* = 8.83 Hz, 2H), 7.94 (m, phenyl-COOH, 4H), 8.65 (s, N=CH, 1H); MS, *m/z* (%) 268.11 (100%) [M–H][–], 537.19 (10%) [2M–H][–]. BNCC: ¹H NMR (DMSO-*d*₆), δ = 7.21 (m, phenyl-N, 1H), 7.24 (m, phenyl-N, *J* = 7.39 Hz, 2H), 7.37 (m, phenyl-N, *J* = 7.17 Hz, 2H), 8.01 (m, phenyl-COOH, 4H), 8.63 (d, N=CH, 1H); MS, *m/z* (%) 224.02 (100%) [M–H][–], 449.17 (6%) [2M–H][–].

3. Sample Preparation. Prior to each adsorption experiment, the GaAs (100) surfaces of the samples were cleaned by boiling them for 15 min in each of trichloroethylene, acetone, and absolute ethanol, successively, then etching them for 10 s in 1:9 NH₃/H₂O (v/v) solution, washing them in deionized water, and drying in a flow of N₂. They were then immersed overnight in a 2–3 mM acetonitrile solution of DMNC, EONC, BNCC, and CNCC or in a 1:1 acetonitrile/1,4-dioxane solution of NCCC. The samples were taken out and carefully rinsed in acetonitrile (in 1,4-dioxane for NCCC). The samples were kept in an evacuated container at room temperature for at least 2 days. Au contacts were deposited on the modified surface in a “soft” manner, using the so-called “lift-off, float-on” technique (LOFO), so as not to damage the molecules on the GaAs surface.³⁷ Au dots, 60 nm thick and 0.5 mm in diameter, were evaporated onto clean glass slides, from which they were allowed to peel by dipping the slide at an angle in 5% (v/v) solution of HF in acetonitrile. The solvent was then changed to pure acetonitrile, which contained the modified GaAs crystal; 0.5–1% (v/v) water was added to increase the surface tension, to allow the Au leaves to float. The GaAs was then lifted out of the solution with the Au on top of it, and the samples were dried for at least 2 days in a vacuum. Wafers of undoped n-GaAs (100) were used to characterize the molecules on the GaAs surface using FTIR, ellipsometry, and contact angle measurements. n-GaAs (100) wafers, Si-doped to $\sim 10^{18}$ cm^{–3}, were used for electrical measurements, as use of relatively highly doped GaAs assured reproducible preparation of good ohmic back contacts.

DFT Calculations. Calculations of dipole moments were carried out using the Gaussian 98 package.³⁸ The B3LYP (Becke 3-parameter hybrid exchange^{39a} with Lee–Yang–Parr correlation^{39b}) density functional theory (DFT) method was used with Dunning’s cc-pVDZ (correlation consistent polarized valence double- ζ ⁴⁰) basis set, which is a [3s2p1d/2s1p] contraction of a [9s4p1d/4s1p] primitive set. Performance and basis set convergence of the B3LYP DFT method for molecular dipole moments was investigated previously⁴¹ and found to be comparable in quality to sophisticated ab initio methods. The results were found to converge if a basis set of [4s3p2d1f] quality was used. For a [3s2p1d] basis set, some basis set incompleteness error was found but definitely not enough to affect any qualitative trends relevant for the present project. All geometries were optimized at the B3LYP/cc-pVDZ level.

Differences with Earlier Work. Optimizing conditions for work with the molecules given in Scheme 1 necessitated some changes in the experimental conditions, used by us earlier.^{10,42a}

TABLE 1: FT-IR Spectral Maxima (cm⁻¹) for the Compounds Adsorbed on n-GaAs^a

compounds (Scheme 1)	$\nu^{\text{as}}\text{CH}$	$\nu^{\text{s}}\text{CH}$	ν^{COOH}	$\nu^{\text{as}}\text{COO}^-$	ν^{aromatic}	$\nu_{\text{X=Y}}^b$	$\nu^{\text{s}}\text{COO}^-$	$\nu_{\text{C-O}}$
DMNC	2963.4 (2971.8)	2856.9 (2874.9)	(1683.1)	1667.0	1633.9 (1594.5,1515.1)	1412.7 (1391.2)	1383.4	1109.9 (1077.6)
EONC	2966.2 (2973.6)	2874.9 (2872.9)	(1680.1)	1656.1	1615.3 (1623.5,1589.9)	1511.3 (1499.7)	1381.3	1065.6 (1047.1)
BNCC			(1679.8)	1667.5	1633.0 (1616.7,1566.4)	1445.2 (1421.5)	1380.4	1108.4 (1115.6)
CNCC			(1686.8)	1669.8	1618.8 (1601.7,1563.4)	1458.0 (1421.1)	1382.2	1105.9 (1109.6)
NCCC			(1682.8)	1666.9	1624.4 (1600.5,1508.6)	1460.2 (1425.8)	1382.8	1108.7 (1104.9)

^a Values for same compounds in KBr are given in parentheses. ^b C=C for NCCC and CNCC, C=N for EONC and BNCC, and N=N for DMNC.

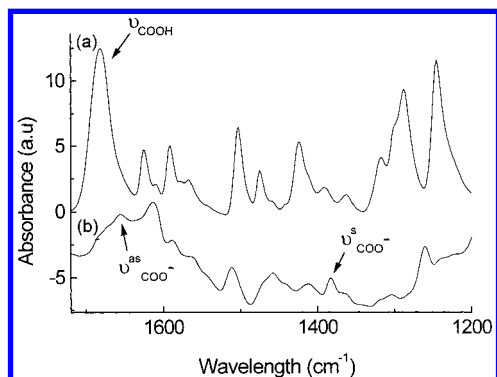


Figure 2. FTIR spectra of EONC (molecule [b] in Scheme 1); (a) in KBr, (b) adsorbed on the surface of n-GaAs (100).

Thus, although GaAs wafers were earlier etched by Br₂/methanol solutions, here we used NH₃/H₂O solutions as the Br₂/methanol one was found to easily damage the GaAs surface.

Reproducibility problems with the Au dot/semiconductor could often be traced to the possibility that solvent molecules remained inadvertently in the interface after LOFO, something that can be expected to affect the electronic properties of the diode. We found that, if the devices were kept in a vacuum (10⁻² Torr) for at least 2 days after they were taken from the adsorption solution and rinsed by solvent, stable devices resulted in a reproducible fashion. Probably this leaves some voids between the Au and the GaAs surface, with direct contact apparently mainly at pinholes. The lack of intimate, direct molecule/Au contact is important for the nature of the diode that forms.^{42b}

Results and Discussion

1. Characterizations of Molecular Layers. *FTIR.* To increase absorbance signals for the molecular film on the surface of the semiconductor, reflection FTIR was used. The main assignments of the spectral features are listed in Table 1 for the compounds on a single-crystal n-GaAs (100) surface and in KBr pellets (brackets). Figure 2 shows typical FTIR spectra of EONC from 1700 to 1200 cm⁻¹. Our main interest is in looking for changes in the binding group spectrum, i.e., for a change in the chemical state of the carboxylic groups. The strong carboxylic absorption bands seen for the free molecules (ν^{COOH} = 1680 cm⁻¹) mostly disappear after molecule adsorption on the n-GaAs (100) surface, whereas new bands appeared at 1656 and 1381 cm⁻¹. They correspond to $\nu^{\text{as}}\text{COO}^-$ and $\nu^{\text{s}}\text{COO}^-$, respectively, indicating that most of the carboxylic groups bind to the GaAs surface as unidentate carboxylate.¹⁴ For all of the compounds, similar intensities were found of the $\nu^{\text{as}}\text{COO}^-$

TABLE 2: Film Thickness (Calculated from Ellipsometry and from Molecular Modeling) and Advancing Contact Angle, for Molecularly Modified n-GaAs Surfaces^a

compounds (see Scheme 1)	film thickness from ellipsometry (Å)	film thickness from molecular model (Å) ^b	contact angle (°) ^c (advancing)
DMNC	14 (2)	15.5	68
EONC	10 (2)	15.5	64.5
BNCC	15 (2)	13.5	57.5
CNCC	13 (2)	15	47
NCCC	15 (2)	13	44

^a All ellipsometry and contact angle measurements are the average for data, obtained from three samples, each of which was measured several times. ^b Based on our computed B3LYP/cc-pVDZ geometries. ^c The contact angle of the reference surface [GaAs in ambient air] is 41.2°.

absorbance peaks, about 7×10^{-4} OD units (0.15% absorption) comparable to earlier results of ours.^{16,20} The procedure is explained in ref 16 for simple benzoic acid derivatives. This indicates that a film of 0.5–1 monolayer is formed by each of the compounds on the GaAs substrate. Aromatic vibrations give a strong broad band after adsorption. As can be seen from Table 1 and Figure 2, the peaks ascribed to the stretching vibrations of the bridge's double bonds ($\nu_{\text{X=Y}}$) and, to a lesser extent, also for the aromatic vibrations are shifted to longer wavelength in the monolayer than in KBr. This may be due to intermolecular interactions in the molecular film (cf. Figure 4 in ref 15).

Ellipsometry. The experiments were performed in air, at incidence angles of 55°, 60°, and 65°. Film thicknesses were extracted using a three-layer model, for the molecular film and the native oxide, with refractive index $n = 1.4$ for the molecular film⁴³ and $n = 2.37$ for that of the native oxides.⁴⁴ For GaAs, 3.8475 and -0.217 were used for the real and imaginary components of the refractive index, respectively.^{44,45} By using the same refractive index values for all of the films, the relative thicknesses of the different layers could be compared. With this model, the oxide thicknesses were found to be about 20–25 Å. For all molecular films, this procedure yielded a thickness close to the calculated height of the molecule. The lower value for EONC may be due to a stronger average tilt of the molecules (from the surface normal) and/or more disorder in the layer.¹⁵ In Table 2, we give both the experimental (average value for three samples) and calculated values.

Contact Angle. The presence of molecules on the n-GaAs wafers, after adsorption, was verified via contact angle determination, using a water drop on the sample surface. Three samples were measured for each compound, and a minimum of three readings for advancing and receding angles were recorded for each sample. The advancing angle data are given

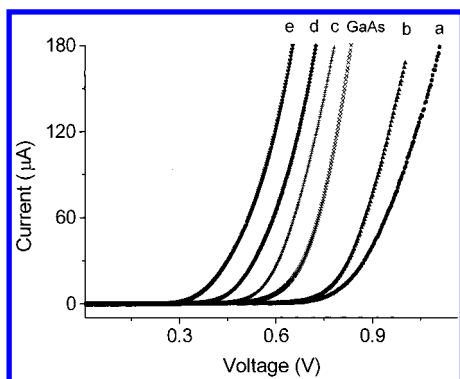


Figure 3. Current–voltage (I – V) curves of Au/n-GaAs diodes, made with n-GaAs crystals that were molecularly modified by adsorbing the conjugated molecules of Scheme 1 onto them. The diodes were made using the LOFO technique.³⁷ “GaAs” stands for the curve obtained with “bare”, i.e., only air-oxidized GaAs.

in Table 2. As expected, the angles are smallest for layers made with the most hydrophilic molecules, CNCC and NCCC. Hysteresis between advancing and receding angles was highest for the more hydrophobic films, DMNC and EONC. This can indicate that films of those molecules are less homogeneous than the others. Such effects lead to effective dipole values, less than those of the isolated molecules, as will stronger average tilt of the molecules.

2. Metal/Semiconductor Diodes. If the free surface is made into an interface, for example by depositing a metal on the molecularly modified surface, then the presence of a dipole layer can affect the barrier height of the resulting metal/semiconductor junction. Referring again to Figure 1, in such a junction the barrier height (ϕ_b) and band bending (V_b) will change according to the molecular layer's dipole.

The barrier height of metal–semiconductor diodes can be extracted from their current–voltage curves in the dark. These were measured in the blocking voltage range, from -1.0 to $+1.0$ V for Au/n-GaAs junctions, modified by BNCC, CNCC, and NCCC molecules, from -1.5 to $+1.5$ V for those modified by DMNC and EONC molecules. For each molecule, several samples were prepared, on each of which three different contact pads were used, with about four measurements per pad. No obvious changes were seen between successive measurements. Each curve in Figure 3 is representative of several measurements. For comparison, diodes prepared on n-GaAs (100) that had been immersed in pure solvent, after cleaning and etching, were measured, too (“bare”). Because the free surface was exposed to air during measurement, this is an oxidized surface. This is important because oxidation increases with time of air exposure.¹⁶ However, we find that once the molecules are adsorbed on the GaAs surface oxidation is halted. For example, after keeping two GaAs samples for 2 days in the moderate vacuum, used here (see above), the bare one had a 4.5 nm thick oxide film, whereas for the one with molecules adsorbed on it, the oxide thickness was found (from ellipsometry) to be only 2.5 nm.

It can be seen from Figure 3 that the I – V curves shift to lower voltage in the following order: DMNC \rightarrow EONC \rightarrow n-GaAs \rightarrow BNCC \rightarrow CNCC \rightarrow NCCC. This indicates that, for a given forward bias voltage, adsorption of molecules with electron-donating substituents decreases the (forward) current, whereas the use of molecules with electron-withdrawing ones increases it, in comparison to “bare” diodes.

Current transport is due principally to minority carriers in p–n junctions but due to majority carriers in metal/semiconduc-

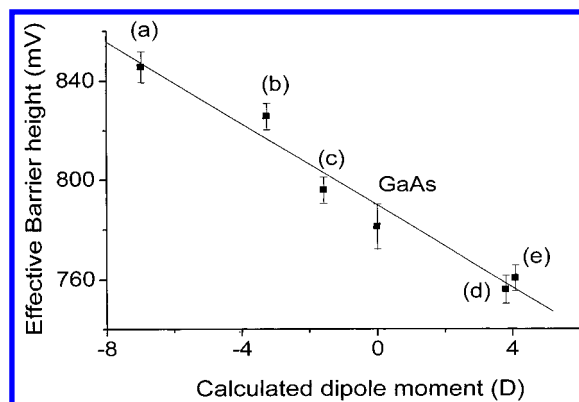


Figure 4. Relationship between the barrier height (ϕ_b in Figure 1), derived from the data of Figure 3, of the molecularly modified Au/n-GaAs interface and the calculated dipole moment of the molecules, shown in Scheme 1.

tor ones. Thus, for metal contacts to n-semiconductors, electrons are the dominant carriers. Thermionic emission over the barrier at the metal–semiconductor interface may be described by⁹

$$J = J_s [\exp(qV/nkT) - 1] \quad (1)$$

where J_s is the saturation current, q is the absolute electron charge, k is the Boltzmann constant, and T is the absolute temperature (here $T = 298$ K). n is the ideality factor which describes the departure of practical diodes from the pure thermionic emission model, e.g., because of image-force barrier lowering. If the current–voltage curves are plotted using semilogarithmic coordinates, a linear variation of $\log(J)$ with V is seen over the 0–0.5 V forward bias range (not shown). The deviation from linearity at higher forward bias voltages (1 V for BNCC, CNCC, and NCCC; 1.5 V for DMNC and EONC) mirrors the potential drop due to ohmic losses in the bulk of the semiconductor. The saturation current is then determined by extrapolating the linear part of the semilog current–voltage plot to zero bias. According to thermionic emission theory, J_s is defined as⁹

$$J_s = A^* T^2 \exp(-q\phi_b/kT) \quad (2)$$

where A^* is the Richardson constant, $4 \text{ A cm}^{-2} \text{ K}^{-2}$ for n-GaAs. The nominal contact area of the Au pads used is $\sim 2 \times 10^{-3} \text{ cm}^2$. The barrier height, ϕ_b , can now be extracted from the 0–0.5 V range of the current–voltage characteristics, using eqs 1 and 2. The values of the barrier height range from 0.75 to 0.85 V (see Figure 4). Relatively high values of the ideality factor are found ($n = 1.3$ – 1.6), which can be attributed to recombination in the space charge layer, owing to a high concentration of traps.⁴⁶ This indicates that thermionic emission may not be the dominating process. In fact, the saturation current can be composed of various parallel currents such as thermionic emission, recombination, tunneling, and injection of holes. (Strictly speaking, ϕ_b should be viewed as an effective barrier height, rather than the true value for pure thermionic emission).

3. Relation between Barrier Height and Dipole Moment. The junction's barrier height (ϕ_b) can be influenced by the interface dipole (μ) at the GaAs–Au contact. The original Schottky–Mott description of Schottky barriers on n -type semiconductors predicts the barrier height to be the difference between the semiconductor electron affinity (χ_s) and the metal work function (ϕ_m). The work function is characteristic for a given surface of a material, which changes with changes in the

surface dipole.^{47,48} We can view χ_s as the sum of a constant (χ_s^0) and a dipole (φ_d) contribution. The net barrier height is then given by (cf. Figure 1)

$$\varphi_b = \varphi_m - (\chi_s^0 + \varphi_d) \quad (3)$$

Here φ_d is the potential step due to the interface dipole

$$\varphi_d = N\mu(\cos \theta)/\epsilon\epsilon_0 \quad (4)$$

where μ is the dipole moment (in units of C m), N is the surface density of dipoles (in m^{-2}), tilted at an (average) angle θ from the normal to the surface, ϵ is the film's effective dielectric constant (which, because we are dealing with a monomolecular layer, may be best interpreted, using the Clausius-Mosotti relation, in terms of molecular polarizabilities), and ϵ_0 is the dielectric permittivity of vacuum.

In forming a planar bonded interface between a metal and a semiconductor, charge transfer will equilibrate the chemical potentials of the two materials. In this context we emphasize that it is the intrinsic semiconductor chemical potential that is relevant to the bond formation process. Schottky barrier heights are controlled by the magnitude of the interfacial bond charge dipole formed at the interface.⁴⁹ The effect of an interface dipole was verified experimentally, using both nonmolecular⁵⁰ and molecular modifications, with the latter allowing for better control.^{10,22}

To see in how far the present molecules fit this description, we performed ab initio calculations of the molecules' dipole moments, using density functional theory (DFT). DFT has been shown to give accurate geometries and other molecular properties.⁵³ During the calculation, we assumed that all of the molecules are in the trans conformation and, for simplicity, the ethyl group in the DMNC and EONC molecules was replaced by a methyl one. The highest negative dipole value was found for molecules with a $(\text{CH}_3)_2\text{N}-$ (donor) group (dipole oriented towards the GaAs surface) and the highest positive dipole for those with an NO_2 (acceptor) group (dipole oriented away from the GaAs surface). Using the same method, excellent agreement was found between calculated and experimental values (in nonpolar solvent or in the gas phase) for benzoic acids, molecules with known dipole moments.⁵¹ The molecular dipole moments that we found were, NCCC (+4.1) > CNCC (+3.8) > BNCC (−1.6) > EONC (−3.3) > DMNC (−7.0).

The DFT calculations show that if we replace the $\text{CH}=\text{CH}$ or $\text{N}=\text{N}$ bonds by an $\text{N}=\text{CH}$ bond the molecule's dipole moment changes by about ~5–10%. For example, calculated dipole moments for EONC and its analogues are −3.8, −3.25, and −3.75 D, if the central double bonds are $\text{N}=\text{N}$, $\text{N}=\text{CH}$, and $\text{CH}=\text{CH}$, respectively. Thus, we conclude that the effect of changing the bridge double bond (which was done for synthetic chemical reasons) does not significantly affect the overall dipole moment and, most importantly, does not affect the order of the dipole moments of the molecules in Scheme 1.

Figure 4 shows the relation between the barrier height of the Au/n-GaAs interface, calculated from the experimental current–voltage characteristics and the ab initio calculated dipole moment. The error bars in all of the plots come from the standard deviations of the measurements. As predicted from eqs 3 and 4, the more positive the dipole, the higher the work function of GaAs, and the smaller φ_b .

4. Relation between the Interfacial and Free Surface Effects of the Molecules. To further understand the effect of the adsorbed molecules, the contact potential difference of the

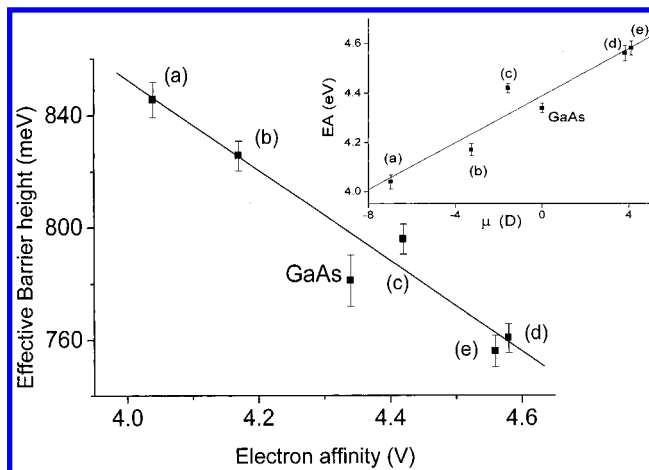


Figure 5. Barrier height (φ_b in Figure 1) of the Au/n-GaAs interface as function of the measured n-GaAs electron affinity (χ_s in Figure 1), after molecular modification with the molecules of Scheme 1. Insert: Electron affinity (χ_s in Figure 1) of n-GaAs, as function of the calculated dipole moment of molecules, adsorbed onto its surface.

n-GaAs (100) surface covered with the monolayers was measured in ambient condition after adsorption. Although the barrier height controls the electrical behavior across a metal/semiconductor interface, the CPD controls the electrical behavior of a semiconductor's free surface.

Figure 5 shows the relation between the barrier height of the Au/molecule-on-n-GaAs interface and the electron affinity of the molecularly modified n-GaAs. The junction's effective barrier height decreases with increasing electron affinity and vice versa. Donor molecules decrease, whereas acceptor molecules increase the n-GaAs electron affinity, which fits with eq 3, because the higher the electron affinity, the smaller the effective barrier height. This supports earlier work,¹⁰ in that it shows that free surface effects can control what happens when the surface is transformed into an interface.

In the insert to Figure 5, we show directly the dependence of the electron affinity on the calculated dipole moment of the adsorbed molecules. The roughly linear relation between the electron affinity and the dipole moment agrees with the prediction of eq 4 and with earlier results of ours.^{14–16,20,21} It also suggests that, notwithstanding the low thickness deduced for EONC (from ellipsometry) and the higher hysteresis in contact angle for EONC and DMNC, there are no major differences in results for films made with these layers, compared to those obtained for samples made with the other molecules. The more positive the molecules' dipole moment, the larger is the semiconductor's effective electron affinity. With $-\text{NO}_2$ and $-\text{CN}$ ($\text{R}_2\text{N}-$ and $\text{RO}-$) groups the adsorbed molecule's dipole has its negative monopole point away from (toward) the semiconductor surface, resulting in an increase (decrease) in surface potential of the semiconductor. As expected, surfaces modified with the nonsubstituted BNCC molecule yield electron affinities between those of surfaces modified with donor-containing and those modified with acceptor-containing molecules.

Differences between the dark work function and the electron affinity are due to band bending (BB) of the modified semiconductor. The BB values extracted from Kelvin probe measurements change only slightly from molecule to molecule (see Table 3), suggesting that BB is primarily determined by GaAs doping and Ga–O surface bonds. A possible trend for acceptor molecules to decrease BB, as compared with bare n-GaAs, maybe understood on the basis of interactions between

TABLE 3: Work Functions and Barrier Heights of Molecularly Modified Free Surfaces and Au/n-GaAs Junctions

compounds (see Scheme 1)	barrier height (mV)	work function ^a (eV)	band bending (mV)
DMNC	845 ± 6	4.35 ± 0.03	300
EONC	830 ± 5	4.55 ± 0.02	350
GaAs	780 ± 12	4.70 ± 0.015	350
BNCC	800 ± 5	4.75 ± 0.02	350
CNCC	760 ± 5	4.80 ± 0.03	200
NCCC	755 ± 5	4.85 ± 0.03	250

^a Versus Au. The WF of Au was taken to be 5.00 eV.

TABLE 4: Comparison of Changes in Barrier Height, in Electron Affinity and in Dipole Moment for Molecularly Modified n-GaAs Surfaces and Au/n-GaAs Junctions, Obtained with Different Series of Molecules^a

	max. ΔBH (mV)	max. ΔEA (meV)	$\Delta\mu$ (Debye)	$\Delta\text{BH}/\Delta\mu$ (mV/D)	$\Delta\text{EA}/\Delta\mu$ (meV/D)
this work	90	540	11	~8	~40
dicarboxylic acids ¹⁰	80	800	7.6 ^b	~11	~100
benzoic acids ^c		950	7.2		~140

^a Compared to n-GaAs free surfaces and n-GaAs/Au junctions.

^b Based on dipole moments for the dicarboxylic acids (tartrate) derivatives,⁵² used in refs 10 and 12. ^c Data are from ref 16. For dipole moments, see ref 51. No Au/n-GaAs devices were as yet reported with these molecules.

the free molecules' LUMO energies and GaAs surface state levels, as explained previously for dicarboxylic acid derivatives with GaAs and other semiconductors.^{12,13} However, until experimental measurements and/or reliable theoretical calculations of these levels become available, such explanation remains speculative.

In comparing the present results with earlier ones, we need to keep in mind the differences between the series of molecules used here and earlier. Because we wish to look for a difference in the systematic trend, we use eq 4 and specifically the slope of EA vs dipole moment plots (as in Figure 5 insert), $\Delta\text{EA}/\Delta\mu$. The slope will reflect differences in density of dipoles, in average tilt of the molecules, and in effective dipole moment/molecule.

Table 4 shows data from this work and that of the earlier Au/dicarboxylic acid-modified n-GaAs¹⁰ system, as well as for the benzoic acid/GaAs surfaces. Considering the above-mentioned caveat, we look for clear-cut differences. FT-IR data do not suggest any drastic differences in coverage between the molecules and as compared to benzoic acids.

In comparing the present data with those for dicarboxylic acids, we need to consider the higher density of the monocarboxylate molecules, because of their smaller footprint (~25 Å²) than that of the dicarboxylates (~40 Å²). This should actually increase the $\Delta\text{EA}/\Delta\mu$ value of the monocarboxylates by a factor of 1.6. This fits roughly the difference between the benzoic and dicarboxylic acids but is opposite to what is seen if we compare the present series with the benzoic or dicarboxylic acids. If the differences in the change in EA/unit dipole moment were due to differences in coverage, this would mean that the present molecules cover only 1/3 of the surface area covered by those used earlier, which should have been seen experimentally (from FTIR experiments, especially)^{15,19,25} Although for the present molecules we have indication of significant average tilt only for the EONC molecules, for the dicarboxylic and benzoic acid layers on GaAs, an average tilt of ~50° was found. Such tilt

would increase the $\Delta\text{EA}/\Delta\mu$ values given in Table 4 by a factor of 1.25–1.4.

Thus, even considering all of these factors it is clear that the $\Delta\text{EA}/\Delta\mu$ value for the present series is significantly smaller (at least by a factor of 2–3) than those obtained with the other series of molecules.

Therefore, we conclude that the low $\Delta\text{EA}/\Delta\mu$ value for the present series of conjugated molecules stands out. The simplest explanations for this are (1) the difference in distance of the dipole groups from the GaAs surface. Although the dicarboxylic acid derivatives give layers 0.9–1 nm thick and the benzoic acid derivatives give 0.7–0.9 nm, layers of the molecules used here are 1.4–1.5 nm thick. All other factors being equal, the dipole effect seen should be strongest with molecules that have their polar groups farthest away from the surface.¹⁹ That is opposite to what we find. (2) Upon binding to the surface, the effective dielectric constant has increased (compare eq 4), and thus, the change in surface potential per dipole moment unit decreases. This increase in effective dielectric constant can be understood on an atomic scale via the Clausius–Mosotti relation from the increased polarizability of the conjugated systems, as compared to the benzoic acid and especially the partially aliphatic dicarboxylic acid ones. The alternative idea, sometimes voiced,²⁶ that a conjugated bridge can be effective for use of electrostatic signal transfer appears not to be applicable here.

If further experiments bear out the $\Delta\text{EA}/\Delta\mu$ differences seen here, then future work that aims at achieving maximal molecular control over semiconductor surfaces should concentrate on mostly σ -bonded systems. The observed difference in $\Delta\text{BH}/\Delta\mu$ is much smaller than $\Delta\text{EA}/\Delta\mu$, suggesting that other effects may come into play when the surface becomes an interface. Possibly the dielectric constant/polarizability effect is stronger at an interface, in a constrained environment. However, such ideas are at present speculative ones only, and extending our tentative conclusions to interfaces awaits further work.

Summary

The electron affinity of a molecularly modified semiconductor surface scales with the dipole moment of adsorbed conjugated molecules with the same binding group and comparable bridging groups. Also, the barrier height of the Au/n-GaAs junction, after molecular modification of the GaAs, can be tuned by changing the dipole moment of adsorbed conjugated molecules. Compared with previous work, the effects are weaker, something that can be ascribed to the higher polarizability of the conjugated system.

Acknowledgment. We thank Ayelet Vilan for her help throughout this work, especially with the ellipsometry and contact angle measurements. We thank the Israel Science Foundation for partial financial assistance. J.M.L.M. is the incumbent of the Helen and Milton A. Kimmelman Career Development Chair.

References and Notes

- (1) Chamberlain, G. A. *Solar Cells* **1983**, 8, 47.
- (2) Kanicki, J. *Handbook of Conducting Polymers*; Skotheim, T. A., Ed.; Marcel Dekker: New York, 1985; Vol. 1.
- (3) Horowitz, G. *Adv. Mater.* **1990**, 2, 287–292.
- (4) (a) Schon, J. H.; Kloc, Ch.; Batlogg, B. *Science* **2000**, 288, 2338; *Nature* **2000**, 406, 702; 408, 549.
- (5) Sirringhaus, H.; Tessler, N.; Friend, R. H. *Science* **1998**, 280, 1741.
- (6) (a) Miller, E. K.; Yang, C. Y.; Heeger, A. J. *Phys. Rev. B* **2000**, 62 (11), 6889. (b) McGehee, M. D.; Heeger, A. J. *Adv. Mater.* **2000**, 12 (22), 1655.
- (7) Packan, P. A. *Science* **1999**, 285, 2079–2081.

- (8) Coronade, E.; Galan-Mascaros, J. R.; Gomez-Garcia, C. J.; Laukhin, V. *Nature* **2000**, *408*, 447–449.
- (9) Sze, S. M. *Physics of Semiconductor Devices*; Wiley: New York, 1981.
- (10) Vilan, A.; Shanzer, A.; Cahen, D. *Nature* **2000**, *404*, 166–168.
- (11) Gartsman, K.; Cahen, D.; Kadyshkevitch, A.; Libman, J.; Moav, T.; Naaman, R.; Shanzer, A.; Umansky, V.; Vilan, A. *Chem. Phys. Lett.* **1998**, *283*, 301–306.
- (12) Cohen, R.; Kronik, L.; Shanzer, A.; Cahen, D.; Liu, A.; Rosenwaks, Y.; Lorenz, J. K.; Ellis, A. B. *J. Am. Chem. Soc.* **1999**, *121*, 10545–10553.
- (13) Cohen, R.; Kronik, L.; Vilan, A.; Shanzer, A.; Cahen, D. *Adv. Mater.* **2000**, *12*, 33–37.
- (14) Bruening, M.; Moons, E.; Yaron-Marcovich, D.; Cahen, D.; Libman, J.; Shanzer, A. *J. Am. Chem. Soc.* **1994**, *116*, 2972–2977. Bruening, M.; Moons, E. D.; Cahen, D.; Shanzer, A. *J. Phys. Chem.* **1995**, *99*, 8368–8373.
- (15) Bruening, M.; Cohen, R.; Guillemoles, J. F.; Moav, T.; Libman, J.; Shanzer, A.; Cahen, D. *J. Am. Chem. Soc.* **1997**, *119*, 5720–5728.
- (16) Bastide, S.; Butruille, R.; Cahen, D.; Dutta, A.; Libman, J.; Shanzer, A.; Sun, L. M.; Vilan, A. *J. Phys. Chem. B* **1997**, *101*, 2678–2684.
- (17) Vilan, A.; Ussyshkin, R.; Gartsman, K.; Cahen, D.; Naaman, R.; Shanzer, A. *J. Phys. Chem.* **1998**, *102*, 3307.
- (18) Ishii, H.; Sugiyama, K.; Ito, E.; Seki, K. *Adv. Mater.* **1999**, *11*, 605–625.
- (19) Evans, S. D.; Ullman, A. *Chem. Phys. Lett.* **1990**, *170*, 462–466. Evans, S. D.; Ullman, E.; Ullman, A.; Ferris, N. *J. Am. Chem. Soc.* **1991**, *113*, 4121–4131.
- (20) Cohen, R.; Bastide, S.; Cahen, D.; Libman, J.; Shanzer, A.; Rosenwaks, Y. *Adv. Mater.* **1997**, *9*, 746–749.
- (21) Cohen, R.; Zenou, N.; Cahen, D.; Yitzchaik, S. *Chem. Phys. Lett.* **1997**, *279*, 270–274.
- (22) Selzer, Y.; Cahen, D. *Adv. Mater.* **2001**, *13*, 508–511.
- (23) Krueger, J.; Bach, U.; Graetzel, M. *Adv. Mater.* **2000**, *12*, 447–451.
- (24) Wu, D. G.; Cahen, D.; Graf, P.; Naaman, R.; Nitzan, A.; Shvarts, D. *Chem. Eur. J.* **2001**, *7*, 1743–1749.
- (25) Hutchison, G. R.; Ratner, M. A.; Marks, T. J.; Naaman, R. *J. Phys. Chem. B* **2001**, *105*, 2881–2884.
- (26) Tour, J. M.; Kozaki, M.; Seminario, J. M. *J. Am. Chem. Soc.* **1998**, *120*, 8486–8493.
- (27) Chen, J.; Reed, M. A.; Rawlett, A. M.; Tour, J. M. *Science* **1999**, *286*, 1550–1552.
- (28) Bumm, L. A.; Arnold, J. J.; Cygan, M. T.; Dunbar, T. D.; Burgin, T. P.; Jones, L., II; Allara, D. L.; Tour, J. M.; Weiss, P. S. *Science* **1996**, *271*, 1705–1707.
- (29) Zhou, C.; Deshpande, M. R.; Reed, M. A.; Jones, L., II; Tour, J. M. *Appl. Phys. Lett.* **1997**, *71*, 611–613.
- (30) Reed, M. A.; Zhou, C.; Muller, C. J.; Burgin, T. P.; Tour, J. M. *Science* **1997**, *278*, 252–254.
- (31) Kergueris, C.; Bourgoin, J.-P.; Palacin, S.; Esteve, D.; Urbina, C.; Magoga, M.; Joachim, C. *Phys. Rev. B* **1999**, *59*, 12505–12513.
- (32) Wu, D. G.; Huang, C.-H.; Huang, Y.; Gan, L.-B.; Yu, A.-C.; Ying, L.-M.; Zhao, X.-S. *J. Phys. Chem.* **1999**, *103*, 7130–7134.
- (33) Wu, D. G.; Huang, C.-H.; Gan, L.-B.; Zheng, J.; Huang, Y.-Y.; Zhang, W. *Langmuir* **1999**, *15*, 7276–7281.
- (34) Walter, H.; Wilhelm, B.; Lothar, F.; Michael, G.; Andreas, G.; Holger, J. Uwe, K.; Norbert, N.; Frank, O.; Hans-Werner, S.; Michael, W. *Makromol. Chem.* **1988**, *189*, 119–127.
- (35) *Organic Syntheses*; Gilman, H., Blatt, A. H., Eds.; John Wiley & Sons: New York, 1958; Vol. 1–9, 374–377.
- (36) Furniss, B. S.; Hannaford, A. J.; Smith, P. W. G.; Yatchell, A. R. *Vogel's Text Book of Practical Organic Chemistry*; Wiley: New York, 1989. Serbutoviez, C.; Bosshard, C.; Knopfle, G.; Wyss, P.; Pretre, P.; Gunter, P.; Schenk, K.; Solari, E.; Chapuis, G. *Chem. Mater.* **1995**, *7*, 1198–1206.
- (37) Moons, E.; Bruening, M.; Shanzer, A.; Beier, J.; Cahen, D. *Synth. Met.* **1996**, *76*, 245–248.
- (38) Frisch, M. J.; Trucks, G. W.; Schlegel, H. B.; Scuseria, G. E.; Robb, M. A.; Cheeseman, J. R.; Zakrzewski, V. G.; Montgomery, J. A., Jr.; Stratmann, R. E.; Burant, J. C.; Dapprich, S.; Millam, J. M.; Daniels, A. D.; Kudin, K. N.; Strain, M. C.; Farkas, O.; Tomasi, J.; Barone, V.; Cossi, M.; Cammi, R.; Mennucci, B.; Pomelli, C.; Adamo, C.; Clifford, S.; Ochterski, J.; Petersson, G. A.; Ayala, P. Y.; Cui, Q.; Morokuma, K.; Malick, D. K.; Rabuck, A. D.; Raghavachari, K.; Foresman, J. B.; Cioslowski, J.; Ortiz, J. V.; Stefanov, B. B.; Liu, G.; Liashenko, A.; Piskorz, P.; Komaromi, I.; Gomperts, R.; Martin, R. L.; Fox, D. J.; Keith, T.; Al-Laham, M. A.; Peng, C. Y.; Nanayakkara, A.; Gonzalez, C.; Challacombe, M.; Gill, P. M. W.; Johnson, B. G.; Chen, W.; Wong, M. W.; Andres, J. L.; Head-Gordon, M.; Replogle, E. S.; Pople, J. A. *Gaussian 98*, revision A.7; Gaussian, Inc.: Pittsburgh, PA, 1998.
- (39) (a) Becke, A. D. *J. Chem. Phys.* **1993**, *98*, 5648. (b) Lee, C.; Yang, W.; Parr, R. G. *Phys. Rev. B* **1988**, *37*, 785.
- (40) Dunning, T. H., Jr. *J. Chem. Phys.* **1989**, *90*, 1007.
- (41) De Proft, F.; Martin, J. M. L.; Geerlings, P. *Chem. Phys. Lett.* **1996**, *250*, 393–401.
- (42) (a) Selzer, Y.; Cahen, D. *Adv. Mater.* **2001**, *13*, 508–511. (b) Vilan, A.; Cahen, D. To be published.
- (43) Lheveder, C.; Meunier, J. In *Physical Chemistry of Biological Interfaces*; Adam, B., Willem, N., Eds.; Marcel Dekker: New York, 2000; pp 559–575.
- (44) Pedinoff, M. E.; Stafsudd, O. M. *Appl. Opt.* **1982**, *21*, 518.
- (45) Aspnes, D. E.; Studna, A. A. *Phys. Rev. B* **1983**, *27*, 985.
- (46) Nishikitani, Y.; Fichou, D.; Horowitz, G.; Garnier, F. *Synth. Met.* **1989**, *31*, 267–273.
- (47) Brillson, L. J. *Contacts to Semiconductors; Fundamentals and Technology*; Noyes: Park Ridge, NJ, 1993.
- (48) Kronik, L.; Shapira, Y. *Surf. Sci. Rep.* **1999**, *37*, 1–204.
- (49) Drummond, T. J. *Phys. Rev.* **1999**, *59*, 8182–8194.
- (50) Capasso, F.; Cho, A. Y.; Mohammed, K.; Foy, P. W. *Appl. Phys. Lett.* **1985**, *46*, 664–666.
- (51) For example, the dipole moments of NO₂–C₆H₄–COOH, H–C₆H₄–COOH, and CH₃O–C₆H₄–COOH are calculated to be 3.54 (3.50), 1.82 (1.72), and –3.52 (–3.67), respectively. The values in parentheses are experimental ones from McClellan, A. L. *Tables of Experimental Dipole Moments*; Freeman: San Francisco, CA, 1963.
- (52) The dipole moments of the dicarboxylic acid (tartrate) derivatives, used in refs 10, 12, 13, and 21 were calculated by the same method as that used here and described in the Experimental Section. For example, (MeO–C₆H₄–COO–CH–COOH)₂ (–4.9D), (CN–C₆H₄–COO–CH–COOH)₂ (+2.7D).
- (53) For reviews, see: Martin, J. M. L. In *Density Functional Theory: a bridge between Chemistry and Physics*; Geerlings, P., De Proft, F., Langenaeker, W., Eds.; VUB Press: Brussels, 2000. De Proft, F. In *Density Functional Theory: a bridge between Chemistry and Physics*; Geerlings, P., De Proft, F., Langenaeker, W., Eds.; VUB Press: Brussels, 2000.
- (54) Cf., for example, Figures 1.3 and 1.10 in Milnes, A. G.; Feucht, D. L. *Heterojunctions and Metal-Semiconductor Junctions*; Academic Press: New York, 1972.